BBA Advances 2 (2022) 100032

Contents lists available at ScienceDirect

BBA Advances

journal homepage: www.sciencedirect.com/journal/bba-advances

Increased phosphorylation of HexM improves lysosomal uptake and potential for managing GM2 gangliosidoses

Graeme Benzie [a,+], Kristen Bouma [a,+], Taylor Battellino [b], Steven Cooper [c], Rick Hemming [c], Wafa Kammouni [c], Lin Liu [d], Cuong Do [d], Mazdak Khajehpour [b], Helene Perreault [b], Stuart Kornfeld [e], Barbara Triggs-Raine [c], Brian L. Mark [a,*]

[a] Department of Microbiology, University of Manitoba, Winnipeg, MB R3T 2N2, Canada
[b] Department of Chemistry, University of Manitoba, Winnipeg R3T 2N2, Canada
[c] Biochemistry and Medical Genetics, University of Manitoba, Canada
[d] M6P Therapeutics, 20 S. Sarah St., St. Louis, MO 63018, United States
[e] Washington University School of Medicine in St. Louis, Department of Biochemistry & Molecular Biophysics, United States

A B S T R A C T

Tay-Sachs and Sandhoff diseases are genetic disorders resulting from mutations in *HEXA* or *HEXB*, which code for the α- and β-subunits of the heterodimer β-hexosaminidase A (HexA), respectively. Loss of HexA activity results in the accumulation of GM2 ganglioside (GM2) in neuronal lysosomes, culminating in neurodegeneration and death, often by age 4. Previously, we combined critical features of the α- and β-subunits of HexA into a single subunit to create a homodimeric enzyme known as HexM. HexM is twice as active as HexA and degrades GM2 *in vivo*, making it a candidate for enzyme replacement therapy (ERT). Here we show HexM production is scalable to meet ERT requirements and we describe an approach that enhances its cellular uptake via co-expression with an engineered GlcNAc-1-phosphotransferase that highly phosphorylates lysosomal proteins. Further, we developed a HexA overexpression system and functionally compared the recombinant enzyme to HexM, revealing the kinetic differences between the enzymes. This study further advances HexM as an ERT candidate and provides a convenient system to produce HexA for comparative studies.

1. Introduction

The GM2 gangliosidoses are a group of lysosomal storage disorders that result from heritable loss-of-function mutations in the α- or β-subunit of the lysosomal heterodimer β-hexosaminidase A (HexA), or in the GM2 activator protein (GM2AP) encoding gene, *GM2A* [1]. Mutations in the α-subunit gene (*HEXA*) result in Tay-Sachs disease; whereas, mutations in the β-subunit gene (*HEXB*) cause Sandhoff disease. HexA degrades GM2 within neurons of the brain and peripheral nervous system with the assistance of a lysosomal protein called GM2AP [2] (for review see [4]). GM2AP extracts GM2 from lysosomal membranes and presents the terminal GalNAc sugar of GM2 to the α-subunit active site of HexA for removal to generate GM3 ganglioside. Loss of HexA activity results in the pathological accumulation of GM2 in neuronal lysosomes, leading to inflammation and cell apoptosis [3], and ultimately to deterioration of motor and cerebral function [4]. The rate of GM2 accumulation depends on how severely mutations reduce HexA activity. Complete loss of HexA activity (<0.5% of wildtype) results in a lethal disorder with onset of clinical symptoms during infancy, whereas mutations resulting in residual activity (1-10% of wildtype) slow GM2 accumulation and lead to juvenile- or adult-onset forms of the disease [5]. Elevated carrier rates of the disease are present among some populations, such as French Canadians of Eastern Quebec with carrier rates as high as 1 in 14 [6] compared to an overall carrier rate of 1 in 206 in Quebec [7], and Ashkenazi Jews who have a carrier rate of ~1 in 31 [8]. The predicted incidence of this autosomal recessive disorder is ~ 1 in 169,668 among all French Canadians in Quebec [7] and ~ 1 in 3900 within the Ashkenazi Jewish population [9]. High carrier rates in some populations have resulted in effective carrier screening programs that have reduced the incidence of disease [6,10]; however, GM2 gangliosidoses remain one of the few high frequency lysosomal storage diseases without a treatment.

Notably, as little as 10% of normal HexA activity could prevent, and possibly reverse, GM2 accumulation and associated clinical phenotypes [5]. This makes ERT [11] and other approaches such as pharmacological chaperones and gene therapy attractive possibilities for managing GM2

* Corresponding author.
E-mail address: Brian.Mark@umanitoba.ca (B.L. Mark).
+ These authors contributed equally to this work

https://doi.org/10.1016/j.bbadva.2021.100032
Received 3 September 2021; Received in revised form 5 November 2021; Accepted 9 December 2021
Available online 13 December 2021

gangliosidoses. To enable an ERT approach, we previously addressed issues of HexA instability and recombinant production that have impeded its use as an ERT by engineering a highly stable variant of the enzyme known as HexM [12]. HexM is designed based on the X-ray structures of human HexA (α/β) and HexB (β/β) [13,14]. Critical features of the α- and β-subunits of these isoforms were identified and combined into a single engineered subunit (μ), which contains the α-subunit active site, the highly stable β-subunit interface, and surface areas that bind to GM2AP [12]. The resulting μ-subunit forms a highly stable homodimer (HexM) that is twice as active as HexA, is endocytosed into lysosomes of deficient cells, and degrades GM2 both *in cellulo* and *in vivo* [12].

To advance the potential of HexM as an ERT candidate to manage GM2 gangliosidoses, we demonstrate that the engineered enzyme is highly stable, and its expression and purification is scalable to levels sufficient for ERT applications. Using the same overexpression system employed for HexM [15], we also developed a recombinant HexA overexpression system and demonstrate comparable kinetic rates with HexM, but with rate constants that reflect the presence of two α-subunits in HexM as opposed to the α/β combination present in HexA. The new expression system for human HexA now provides a convenient source of active enzyme. Further, we show that co-expression of HexM with a highly active and promiscuous engineered version of human GlcNAc-1-phosphotransferase (S1S3 PTase) [16] markedly enhances HexM phosphorylation and its cellular uptake into Tay-Sachs disease fibroblasts. Finally, mass spectrometry-based glycoform analysis reveals that the glycosylation pattern of HexM is consistent with HexA. Together, our studies advance the potential of HexM as a biologic to manage GM2 gangliosidoses and provide a means to conveniently produce HexA for future functional studies and pharmacological chaperone development.

2. Materials and methods

2.1. Materials

The HEKHexABKO cell line as well as the pB-T-RfA, pB-RB and pBase plasmids were provided by Dr. M. Tropak (SickKids Hospital, Toronto). The TSD fibroblasts WG 1881 were obtained from the Human Mutant Cell Repository, Montreal Children's Hospital, the pCDNA6/S1S3 GlcNAc-1-phosphotransferase expression plasmid was provided by M6P Therapeutics (St. Louis, MO), the pCl neo-hEST2 hTERT expression plasmid was from Addgene [17], and the large T-antigen expression plasmid was a gift from Dr. R. Gravel (University of Calgary).

Primers and synthetic DNA fragments were purchased from Integrated DNA Technologies (Coralville, IA). Gateway Cloning reagents were acquired from Thermo Fisher Scientific (Waltham, MA).

The reagents Bis-Tris, citric acid, bovine serum albumin (BSA), polyethylene glycol (PEG) 8000, Triton X-100 and betaine hydrochloride were obtained from Sigma-Aldrich (St. Louis, MO). Imidazole, Tris base, glycerol, sodium chloride (NaCl), potassium dihydrogen phosphate (KH_2PO_4), sodium phosphate dibasic heptahydrate ($NaHPO_4 \bullet 7H_2O$) and sodium phosphate monobasic monohydrate ($NaH_2PO_4 \bullet H_2O$) were purchased from Fisher (Waltham, MA).

Dulbecco's Modified Eagle Medium (DMEM), fetal bovine serum (FBS) and penicillin-streptomycin were purchased from Gibco (Waltham, MA). Doxycycline was obtained from Sigma-Aldrich (St. Louis, MO), while puromycin and blasticidin S were purchased from Invivogen (Waltham, MA). The FiberCell bioreactor, the C2011 cartridges and the Chemically Defined Media for High Density (CDM-HD) serum replacement powder were purchased from FiberCell Systems Inc (New Market, MD). Phosphate buffered saline was obtained from Thermo Fisher Scientific (Waltham, MA) and T75 flasks were acquired from Corning (Corning, NY).

For immobilized metal affinity chromatography, HisPur™ Ni-NTA resin (cat. #: 88222) was obtained from Thermo Fisher Scientific (Waltham, MA). A HiLoad 16/600 Superdex 200 column from GE Life Sciences (Chicago, IL) was used for size exclusion chromatography. The ANTI-FLAG® M2 Affinity Gel (cat #: A2220) was acquired from Sigma-Aldrich (St. Louis, MO).

The substrates 4-methylumbelliferyl 2-Acetamido-2-deoxy-β-D-glucopyranoside (MUG) and 4-methylumbelliferyl 6-Sulfo-2-acetamido-2-deoxy-β-D-glucopyranoside (MUGS) were purchased from Toronto Research Chemicals (North York, Canada), while 4-methylumbelliferone (cat. #: M1381) was obtained from Sigma-Aldrich (St. Louis, MO). The 96-well plates used for kinetic assays were acquired from Corning (Corning, NY).

The anti-HexA Rb polyclonal antibody (cat #: ab91624) and the anti-HexB Rb monoclonal antibody (cat #: ab140649) were purchased from Abcam (Cambridge, UK). Phospho-Tag Phosphoprotein Gel Stain was obtained from ABP Biosciences (Beltsville, MD).

2.2. Protein production

A *HEXA* and *HEXB* knockout HEK293T cell line (HEKHexABKO), lacking endogenous Hex activity, was stably transfected with a HexM expression construct containing a His-tag to generate HEKHexABKO-HexM [12]. The HEK293T cell line was seeded into a FiberCell bioreactor. All cells were grown in DMEM in the presence of 1% Pen-Strep, doxycycline (1 μg/ml), and 10% CDM-HD serum replacement powder. FiberCell Systems Inc. standard protocol was followed for the extraction of media from the bioreactor every two days. His-tagged protein was collected via immobilized metal affinity chromatography. The wash buffer was 10 mM Bis-Tris (pH 6) and 100 mM NaCl (BT buffer). The elution buffer was BT buffer (pH 6) with the addition of 250 mM imidazole. The protein was purified by SEC using BT buffer. Protein was resolved in SDS-PAGE under reducing conditions, transferred to a nitrocellulose membrane, and detected with an anti-HexA Rb polyclonal antibody (1/300 dilution) using the manufacturer's protocol described.

2.3. HexA generation and purification

To produce recombinant HexA that could be separated from other β-hexosaminidase isoforms, double-stranded DNA fragments encoding *HEXA* and *HEXB* were obtained. A two-step PCR was performed using the forward (AAAAAGCAGGCTCCAAAGCCACCATGACAAGCTCC AGGCTTTGG) and reverse *HEXA*-FLAG primers (AGAAAGCTGGG TCTCACTTGTCATCGTCTCCTTGTAATCGGTC TGTTCAAACTCCTG TC), followed by the forward (GGGGACAAGTTTGTACAAAAAAGC AGGC) and the reverse (GGGGACCACTTTGTACAAGAAAGCTGGG) universal *attB* primers to add a C-terminal FLAG-tag and the Gateway cloning *attB* sites to *HEXA*. To add a C-terminal His-tag and the same *attB* sites to *HEXB,* a similar two-step PCR amplification was performed using the forward (AAAAAGCAGGCTCCAAAGCCACCATG-GAGCTGTGCGGGCTGGGG) and reverse *HEXB*-His primer (AGAAAGCTGGGTCTTAATGATGATGATGATGATGTCTA CCCTCGAT-CATGTTCTCATGGTTACA) followed by the forward and reverse universal *attB* primers.

The BP reaction was used to clone the amplified *HEXA* and *HEXB* genes into a Gateway donor vector (pDONR201). The LR reaction was subsequently used to transfer *HEXA* and *HEXB* into pB-T-RfA, a mammalian cell expression plasmid [15]. Both the BP and the LR reactions were carried out as per the manufacturer's instructions. The resulting pB-T-RfA-*HEXA* and pB-T-RfA-*HEXB* constructs were verified by Sanger sequencing (The Center for Applied Genomics, Toronto).

Polyethylenimine (PEI) was used to transfect HEKHexABKO (~4.0×10^6 cells) with 5 μg of pB-T-RfA-*HEXA*, 3 μg of pB-T-RfA-*HEXB*, 1 μg of pB-RB and 1 μg of pBase, the plasmids required for the *piggyBac* transposon-based protein expression system. Transfectants were selected for after 72 hours, using puromycin (10 μg/ml) and blasticidin S (5 μg/ml), which were added to the media [15]. The stably transfected HEKHexABKO-HexA cell line was seeded into a FiberCell bioreactor as

described for HEKHexABKO-HexM.

HexA was purified from the media collected from the FiberCell bioreactor by immobilized metal affinity chromatography, using 10 mM phosphate buffer (5.78 mM $Na_2HPO_4 \bullet 7H_20$, 4.22 mM $NaH_2PO_4 \bullet H_20$; pH 7.0) as the wash buffer and 10 mM phosphate buffer, 250 mM imidazole (pH 7.0) as the elution buffer. The elution fractions were pooled together and dialyzed overnight at 4°C against tris-buffered saline (50 mM Tris-HCl, 150 mM NaCl; pH 7.4). The dialyzed protein was subsequently run through a column containing anti-FLAG affinity resin, using the manufacturer's protocol. HexA production was verified by western blot as described for HexM, using a 1/1000 dilution of the rabbit polyclonal anti-HexA Ab.

2.4. HexM and HexA kinetic assays

The enzyme activity of recombinant HexA was compared to that of HexM using MUG or MUGS as a substrate; hexosaminidases can cleave these substrates and release a highly fluorescent product {4-methylumbelliferone, (4-MU)}, which can be used to assay enzyme activity [18–20]. HexA and HexM were purified as described above and protein concentrations were determined by measuring UV absorbance at 280 nm using a NanoDrop One (Thermo Fisher Scientific). The molecular weight and extinction coefficient of each enzyme were acquired (HexM MW: 125,183 Da and ε_{280}: 216,400 $M^{-1}cm^{-1}$, HexA MW: 124,780 Da and ε_{280}: 233,510 $M^{-1}cm^{-1}$) using the ProtParam tool from ExPASy: SIB bioinformatics resource portal and were taken into consideration when determining protein concentrations.

The enzyme assays were performed in opaque polystyrene 96-well plates (Corning, New York USA). HexM or HexA (final concentration of 100 pM) were aliquoted into each well and either MUGS (0.18 mM, 0.30 mM, 0.42 mM, 0.60 mM, 0.90 mM, 1.20 mM, 1.50 mM, 3.00 mM and 3.50 mM final concentrations) or MUG (0.18 mM, 0.30 mM, 0.42 mM, 0.60 mM, 0.90 mM, 1.20 mM, 1.50 mM, 2.00 mM, 3.00 mM, 3.50 mM and 4.00 mM final concentrations) were added. The total well volume was brought to 100 μl by adding McIlvaine (citrate-phosphate) buffer (pH 4.2) supplemented with w(g)/v(ml) 0.5% bovine serum albumin. Each kinetic assay was performed with three technical replicates and was monitored for 30 minutes at 37°C in a SpectraMax ID5 plate reader (Molecular Devices) by selecting the excitation and emission bandpass at 365 nm and 450 nm respectively. SoftMax Pro software was used to collect the data.

Monitoring hexosaminidase activity with fluorescence presents a unique, often neglected technical challenge; i.e., the predominance of inner-filter effects due to significant substrate absorbance. This problem is circumvented by calculating product concentrations from the degree of conversion (DOC) parameter as defined by Shulman *et al.* (1980) [20]:

$$\mathrm{DOC} = \frac{\mathrm{F(t)} - \mathrm{F(0)}}{\mathrm{F(0)\ x\ 120}}\ \mathrm{x}\ 100\%$$

For a given initial substrate concentration S_0, F(t) is the fluorescence intensity of the reaction mixture measured at time (t) after enzyme addition, F(0) is the fluorescence intensity of the substrate at S_0 concentration (no enzyme present). The DOCs were subsequently used to calculate the concentration of 4-MU ($[P_t]$) released using the following formula:

$$[P_t] = (\mathrm{DOC}) \times S_0$$

Microsoft Excel was used to plot product (Pt) against time in order to determine initial hydrolysis rates. Nonlinear least squares regression analysis required for fitting the resulting data to the Michaelis Menten equation was performed using GraphPad Prism 8.

2.5. Protein phosphorylation analysis

HexM-producing HEK293T cells were transiently transfected with a pCDNA6/S1S3 GlcNAc-1-phosphotransferase (S1S3 PTase) expression plasmid [16], which had the polyHis tag removed. PEI was used to transiently transfect HEKHexABKO-HexM cells with the S1S3 PTase plasmid following a previously established protocol. 20 μg of S1S3 PTase plasmid was mixed with 1 ml serum-free DMEM and 60 μl of PEI and subsequently added to a T75 flask. Media from S1S3 PTase transfected T75 flasks was collected over four days. The expressed protein was a soluble engineered HexM enzyme. Media from S1S3 PTase non-transfected (control) and transfected cells was collected and purified via IMAC and SEC and protein phosphorylation was assessed by Phospho-Tag Phosphoprotein Gel Stain, a highly sensitive fluorescent stain designed to selectively complex its zinc center with phosphate groups, following the manufacturer's protocol.

2.6. Cellular uptake assay

A TSD fibroblasts line WG 1881, that was homozygous for the 7.6 kbp French Canadian deletion [21] was chosen for uptake assays because the *HEXA*-encoded alpha subunit is not expressed. An immortalized form of the cell line (WG 1881) was generated by co-transfection of human telomerase reverse transcriptase (TERT) and the SV40 large T-antigen. To assess the effects of phosphorylation on endocytosis of HexM and hyperphosphorylated HexM (phosHexM), a cellular uptake assay was conducted following a modified version of a previously described protocol [16]. TSD WG1881 cells (1.0×10^6 cells/well) were grown in 6 well plates in Dulbecco's Modified Eagle Medium supplemented with 10% FBS and 1% penicillin and streptomycin. 25 μg of phosHexM or HexM protein was added to each well in the presence or absence of 5 mM mannose-6-phosphate (M6P) or mannose. After 24 hours of growth at 37°C, cells were washed twice with phosphate-buffered saline (PBS; pH 7.4) and then scraped into PBS. The cells were pelleted using centrifugation and then resuspended for 10 minutes on ice in 100 μl of cell lysis buffer (PBS w/v 0.5% Triton-X 100). The cell debris was pelleted by centrifugation (15 mins x 13,000 rpm) and the supernatant was collected and used for the determination of protein concentration and HexM activity. Total protein concentration was determined using a BSA standard curve. HexM activity was assayed using 4-MUGS as a substrate and activity was determined from a 4-methylumbelliferone standard curve. The data was subsequently analyzed using a paired t-test.

2.7. Matrix-assisted laser desorption/ionization mass spectrometry (MALDI-MS)

Measurements by MALDI-MS according to a glycoproteomic approach were conducted in order to determine glycosylation sites and glycan structures in HexM and HexA.

Ammonium bicarbonate, dithiothreitol (DTT), iodoacetamide (IAA), trifluoroacetic acid (TFA), acetonitrile (ACN), and 2,5-dihydroxybenzoic acid (DHB) were purchased from Sigma-Aldrich (St. Louis, MO). C18 cartridges were purchased from Phenomenex (Torrance, CA). Endoproteinase GluC was purchased from New England Biolabs (Ipswich, MA).

HexA, HexM and PhosHexM (100 μg) were suspended in 50 mM ammonium bicarbonate (pH 8.5). Samples were reduced with 10 mM DTT (56°C, 45 min) and alkylated with 50 mM IAA (room temperature, in the dark, 30 min). Excess IAA was quenched by adding 15 mM DTT. Samples were cleaned and fractionated (9 fractions per sample) using C18 cartridges. GluC was added at a 1:50 enzyme to substrate ratio for overnight digestion (16-18 h) at 37°C.

Peptide/glycopeptide fractions were lyophilized and resuspended in 20 μL of 0.1% TFA in 30:70 ACN to water (TA30). They were mixed with DHB matrix solution (20 mg/mL in TA30) at a 1:1 ratio. Each mixture (1 μL) was spotted onto the stainless-steel MALDI target and allowed to dry. The following peptide calibration mixture (American Peptide Company, Vista, CA) was used: bradykinin (1–7) 757.3992; angiotensin II

1046.542; angiotensin I 1296.685; substance P 1346.735; bombesin 1619.822; ACTH clip (1–17) 2093.086; ACTH clip (18–39) 2465.198; ACTH (1–39) 4539.267, where ACTH = adrenocorticotropic hormone and numbers are calculated *m/z* values of $[M+H]^+$ ions. 1 μL of a TA30 solution containing 0.125 μg of each protein was mixed at a 1:1 ratio with DHB matrix solution and spotted onto the target. An UltrafleXtreme™ mass spectrometer (Bruker Daltonics, Bremen, Germany) was used in reflector positive mode for analysis.

3. Results

3.1. Production and purification of HexM and recombinant human HexA

To produce HexM in quantities sufficient for the functional studies described herein, as well as for future structural and preclinical ERT studies, we used a FiberCell bioreactor system to grow a HEK293T cell line (HEKHexABKO-HexM) [12] that secretes overexpressed HexM into the growth medium. Genes *HEXA* and *HEXB* are inactivated in the *HEXA* and *HEXB* knockout HEK293T cell (HEKHexABKO) line, which eliminates endogenous HexA and B expression. HexM (containing a C-terminal His_6 affinity tag) was produced in the cells from expression cassettes that were stably integrated into genome using a *piggy*B*ac* transposon-based system [12,15]. To establish a cell culture for HexM expression, HEKHexABKO-HexM cells were seeded into the extracapillary space (~20 ml) of a C2011 FiberCell bioreactor cartridge. Hollow fibers that run through the extracapillary space of the cartage act like capillaries (20 kDa cutoff) to provide nutrients and remove waste while also providing a large surface area (~4000 cm^2) for cell growth. Previously, cell culture using traditional culture flasks yielded ~ 1 mg/l of HexM-His_6 (1 l of media collected over time from 4 × T75 flasks of cells)

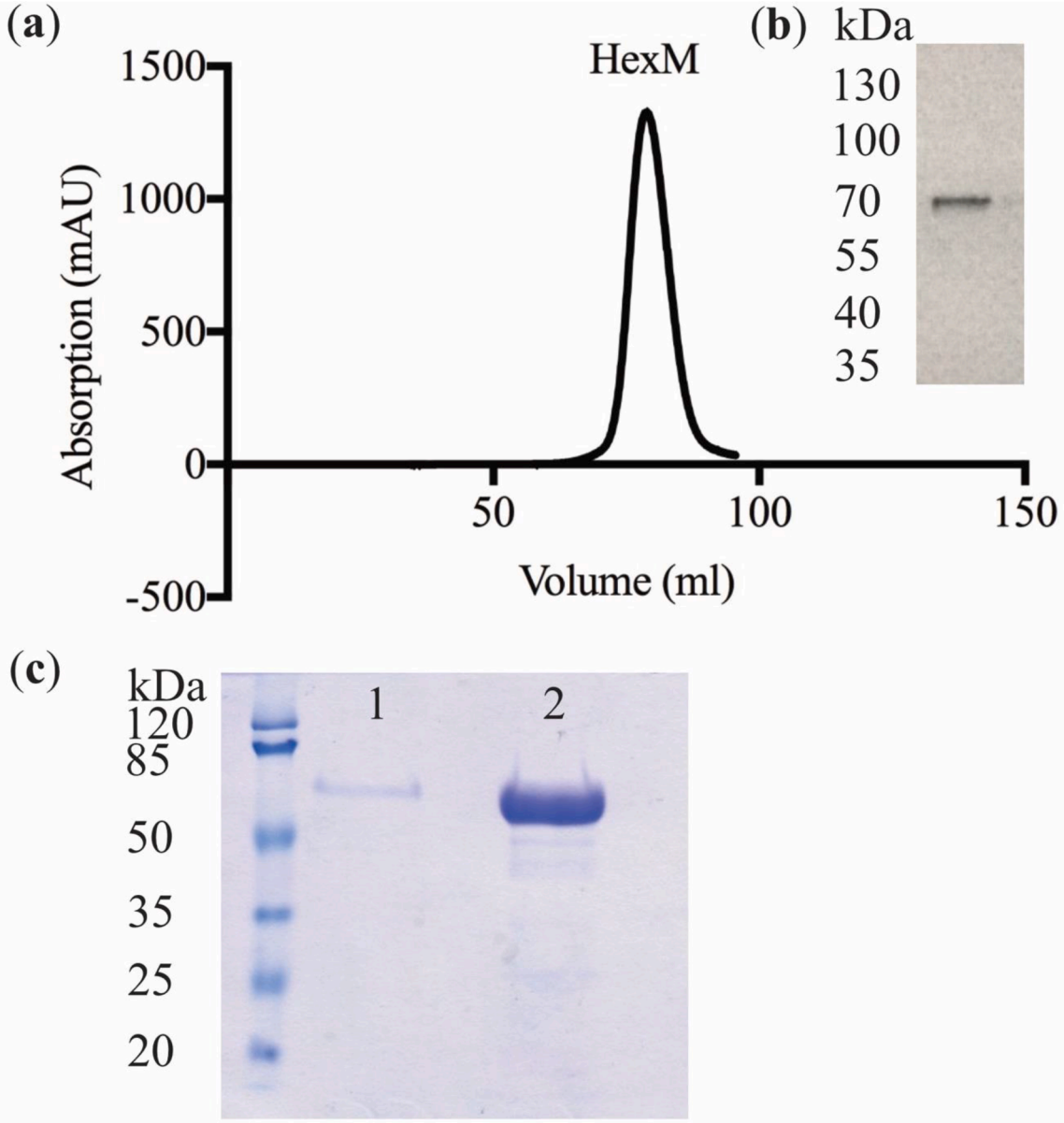

Fig. 1. Purification of HexM from culture medium used to grow HEKHexABKO-HexM cells in a FiberCell bioreactor (a) Elution profile of a HiLoad 16/600 Superdex 200 (GE Life Sciences) gel filtration run with HexM after the protein had been affinity purified from crude extract using a nickel-NTA resin. (b) Western blot of HexM. A 50 μl sample was taken from the peak fractions collected during gel filtration and assessed for the presence of the HexM in its reduced form (~62 kDa). An anti-HexA antibody (ab91624) was used to detect the protein and PageRuler Prestained Protein Ladder (ThermoFisher Scientific) was used as a size standard. (c) Coomassie blue stained SDS-PAGE gel of purified HexM (~62 kDa) produced by HEKHexABKO-HexM cells. Pierce Prestained Protein MW Marker (ThermoFisher Scientific) was used as a ladder. Lane1 is HexM purified from cells grown in a T75 flask. Lane 2 is a purified sample from a FiberCell harvest.

[12]. In contrast, the FiberCell bioreactor proved to be significantly more productive, yielding ~ 2 mg of HexM per daily extraction (~20 ml), yielding ~100 mg/l of culture medium. Approximately 3.5 liters of growth medium was extracted from the FiberCell cartridge (~600 mg of HexM) over 6 months.

Roughly 60 mg of HexM-His_6 produced by the C2011 FiberCell cartridge was purified to demonstrate the robustness of the expression system. The enzyme was found to be highly stable during purification and was readily brought to homogeneity by affinity chromatography using Ni-NTA resin, followed by size exclusion chromatography (HiLoad 16/600 Superdex 200, GE Life Sciences). Western blot analysis and SDS-PAGE confirmed the identity and purity of the enzyme (**Figure 1**).

To our knowledge, a system to generate milligram quantities of human HexA from mammalian cell culture is not currently available. The ability to produce recombinant HexA would provide an excellent control enzyme during development of HexM as an ERT strategy, as well as open further structural and functional studies of the enzyme, including efforts to identify new pharmacological chaperones as treatments for later-onset forms of GM2 gangliosidoses [22]. Thus, we developed a human HexA expression system based on the same *piggyBac* transposon-based system [15] that was used to construct the HexM expression system [12]. As was done for the μ-subunit of HexM, expression cassettes for the α- and β-subunits of HexA were integrated into the genome of the HEKHexABKO cell line. The resulting HexA producing cells (HEKHexABKO-rHexA) were then seeded into the extracapillary space (~20 ml) of a C2011 FiberCell bioreactor cartridge for HexA production.

The bioreactor cartridge provided excellent yields of HexA, producing ~ 0.4 mg of the enzyme per daily extraction (~20 ml), yielding ~20 mg/l of culture medium. Given the combination of isoforms generated when co-expressing the α- and β-subunits (HexA [α/β], HexB [β/β] and HexS [α/α]), the yield of HexA was expected to be lower than HexM, since the latter only adopts one form (homodimer of μ-subunits). HexA was purified by removing the HexB (β/β) and HexS (α/α) isoforms as well as other contaminants using a two-step affinity chromatography procedure (**Figure 2a**). This was achieved by fusing the C-terminus of the α-subunit to a FLAG affinity tag (DYKDDDDK) and fusing a His_6 tag to the C-terminus of the β-subunit. Loading extracapillary media extracts onto a column containing nickel-NTA resin captured proteins of molecular mass consistent with the masses of α- and β-subunits, which were confirmed by western blot (**Figure 2b, c, d**). Protein eluted from the nickel-NTA resin was comprised of both HexA and HexB isoforms since both contained a His_6 tagged β-subunit. HexA was successfully isolated from this mixture using an anti-FLAG immunoaffinity column (**Figure 2a, b**). As described below, in addition to western blotting (**Figure 2c, d**), kinetic analysis of the enzyme eluted from the anti-FLAG column confirmed the enzyme as HexA. The above expression and purification scheme provide more than enough human HexA for functional comparisons to HexM as described below and will enable future structural and functional studies of the enzyme as well as development of pharmacological chaperones of the enzyme.

3.2. Enzymatic characterization of purified HexM and HexA

The enzymatic activities of purified HexM and HexA were compared using the substrate analogues MUG and MUGS. The α- and the β-subunits of human HexA have different affinities towards MUG and MUGS due to the presence of a unique 6-sulfo group on MUGS. The 6-sulfo group imparts a negative charge on the analogue that mimics the negatively charged sialic acid present on the natural GM2 substrate. The α-subunit of HexA is positively charged due to the presence of a basic reside, Arg 424, which enhances its ability to catalyze the hydrolysis of negatively charged substrates such as MUGS and GM2 [23], as well as neutral substrates [18]. In contrast, the β-subunit active site lacks an equivalent

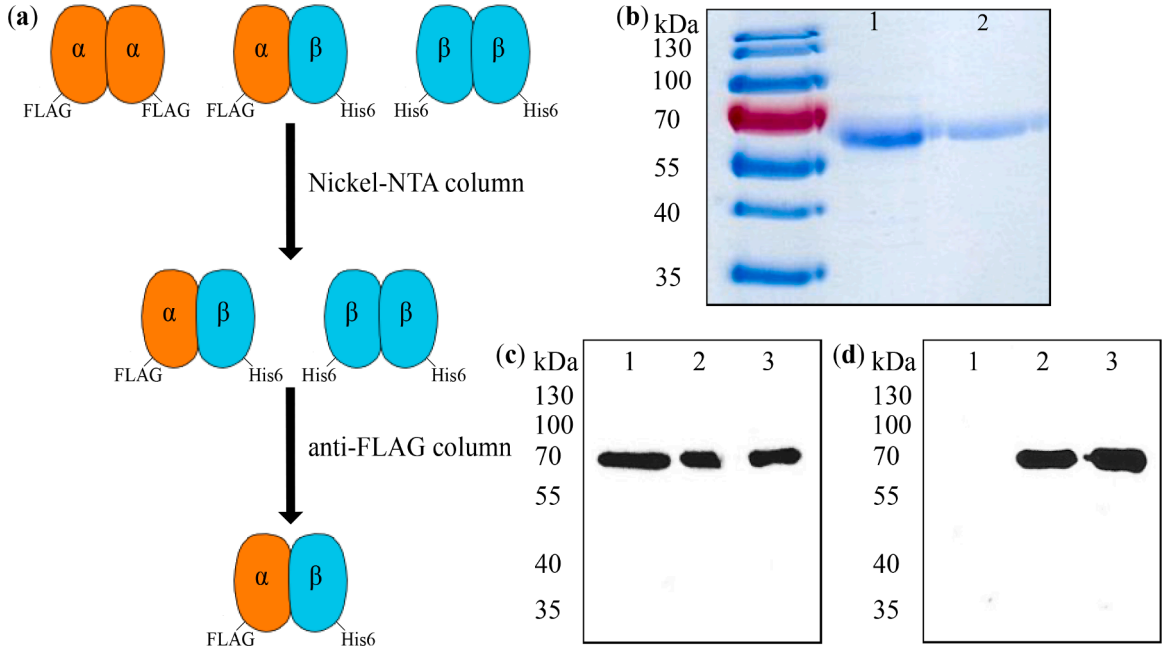

Fig. 2. Purification of recombinant HexA from culture medium used to grow HEKHexABKO-rHexA cells in a FiberCell bioreactor. (a) Two-step purification scheme for rHexA. Cell culture media collected from the FiberCell bioreactor was passed through a column containing nickel-NTA resin, capturing rHexA (α/β) and rHexB (β/β) and removing any rHexS (α/α). Enzyme eluted from the nickel-NTA resin was dialized overnight and passed through a column containing anti-FLAG immunoaffinity resin, which selectively captured rHexA (α/β). (b) SDS-PAGE analysis of rHexA purity (subunits are ~62 kDa). PageRuler Prestained Protein Ladder (ThermoFisher Scientific) was used for the ladder. Lane 1 is the elution fraction from the Ni-NTA column (~3 μg). Lane 2 is an elution fraction from the anti-FLAG affinity resin (~1 μg). Confimation of Hex subunits by western blot analysis using an (c) anti-HexA antibody (ab91624) and an (d) anti-HexB antibody (ab140649). PageRuler Prestained Protein Ladder (ThermoFisher Scientific) was used as a size standard for both western blots. Lane 1 contains 100 ng of purified HexM. Lane 2 contains 100 ng of protein eluted from the Ni-NTA column (HexA and HexB mixture). Lane 3 contains 100 ng of purified HexA, after elution from the anti-FLAG column.

Arg residue within its active site and is much more efficient at hydrolyzing neutral substrates, such as MUG, than negatively charged ones [18,23,24]. Given the different substrate specificities of the α- and β-subunits for MUG and MUGS, the natural Hex isoenzymes and HexM display unique activity profiles.

The catalytic efficiencies of HexM and HexA produced by the FiberCell system were examined by measuring their ability to hydrolyze MUGS and MUG. The kinetic data associated with the hydrolysis of these two substrates follow Michaels-Menten kinetics and the results of this analysis are shown in **Figure 3**. It can be clearly seen that both HexA and HexM enzymes exhibit similar affinities ($K_m \approx 1.25$ mM) towards the negatively charged MUGS substrate; while at the same time, the MUGS turnover number (k_{cat}) for HexM is approximately twice that of HexA. This result is to be expected given that HexM has two α-subunit active sites that are both capable of hydrolyzing the MUGS substrate as opposed to HexA, which only has one. **Figure 3** also shows that relative to HexA enzyme, HexM binds the MUG substrate marginally less tightly and has a reduced turnover number. The observed variance in catalytic parameters is not unexpected, previous work in fact postulates that there are differences in the α-subunit active site when it is present in the heterodimeric versus the homodimeric form [18]. Instead of comparing individual k_{cat} and K_m values, it may be more informative to compare enzyme specificity constants (k_{cat}/K_m) of the two enzymes: 1) Unlike HexA, HexM has equal specificity towards neutral and negatively charged substrates; 2) HexM has twice the specificity of HexA relative to negatively charged substrates; 3) HexM has half the specificity of HexA relative to neutral substrates. This demonstrates that we have successfully combined critical features of the α- and β-subunits of HexA into a single subunit that mimics the properties of both, in order to create the homodimeric enzyme HexM.

3.3. Cellular uptake of HexM is enhanced when it is highly phosphorylated by an engineered GlcNAc-1-phosphotransferase (S1S3 PTase)

We previously engineered a highly active and promiscuous version of human GlcNAc-1-PT (S1S3 PTase) that increases M6P levels on co-expressed recombinant lysosomal proteins to improve their cellular uptake via M6P receptors [16]. To determine if the S1S3 PTase could hyperphosphorylate HexM to enhance its cellular uptake via M6P receptors, we transiently expressed the S1S3 PTase in the HEKHexABKO-HexM cell line and purified HexM from the cells as described above. Compared to HexM isolated from cells that were not co-expressing the S1S3 PTase, phosphorylation of the enzyme was markedly enhanced in the presence the S1S3 PTase when detected using the phosphate-specific binding dye, Phospho-Tag (ABP Biosciences) (**Figure 4a**) and hyperphosphorylation of HexM did not affect enzyme activity (**Figure S1**).

To determine if the enhanced phosphorylation of HexM increased cellular uptake of the enzyme, TSD fibroblast cells WG1881 that completely lack endogenous HexA activity were fed HexM that had been expressed in the absence of the transferase, or HexM that had been hyperphosphorylated by co-expression with the S1S3 PTase. Further, the TSD cells were also fed with the above enzymes in the presence of free M6P or mannose to determine if these free sugars would compete with the enzymes for their respective receptors, thereby providing insight into the specificity of receptor-mediated uptake. After an overnight incubation the cells were washed and uptake was measured by detecting HexM activity in cell lysates using MUGS as substrate (**Figure 4b**). Lysates from cells that had been fed PhosHexM were found to have 3-fold more MUGS activity compared to lysates from cells that had been fed HexM expressed in the absence of the transferase ($p<0.05$, paired t-test). Further, supplementation of the media with free M6P caused the greatest reduction in HexM uptake ($p<0.05$, paired t-test), with relatively little to no reduction in uptake caused by free mannose. The competition posed by free M6P suggests the uptake of PhosHexM is

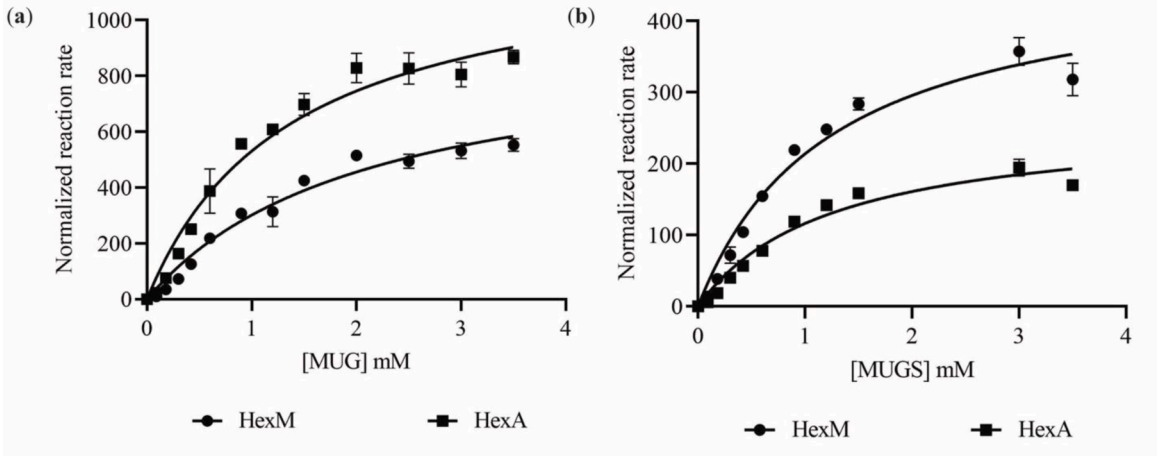

	MUGS		MUG	
Hex isoform	HexM	HexA	HexM	HexA
K_m[a]	1.24 ± 0.15	1.25 ± 0.17	2.10 ± 0.31	1.37 ± 0.17
k_{cat}[b]	479 ± 26	262 ± 16	934 ± 72	1260 ± 67
k_{cat}/K_m[c]	386000 ± 50000	210000 ± 30000	445000 ± 70000	920000 ± 120000

[a] Experiment was performed in triplicate, ± values represent SD. Units for these values are mM. [b] Units are s^{-1}, ± values represent SD. [c] Units for these values are $M^{-1}\,s^{-1}$, ± values represent SD.

Fig. 3. Michaelis-Menten plots of the hydrolysis kinetics of (a) MUG or (b) MUGS by HexM (circles) or recombinant HexA (squares). The normalized reaction rate (NRR) is obtained by dividing the product formation rate by the total enzyme concentration. The assay conditions are defined in the text. Data points represent the average of three technical replicates. The standard deviations are indicated by error bars, for points where the error bars are not shown, the standard deviations fall within the data point dimensions in the graph and the curves represent the best correlation obtained between the Michaelis-Menten equation and the kinetic data.

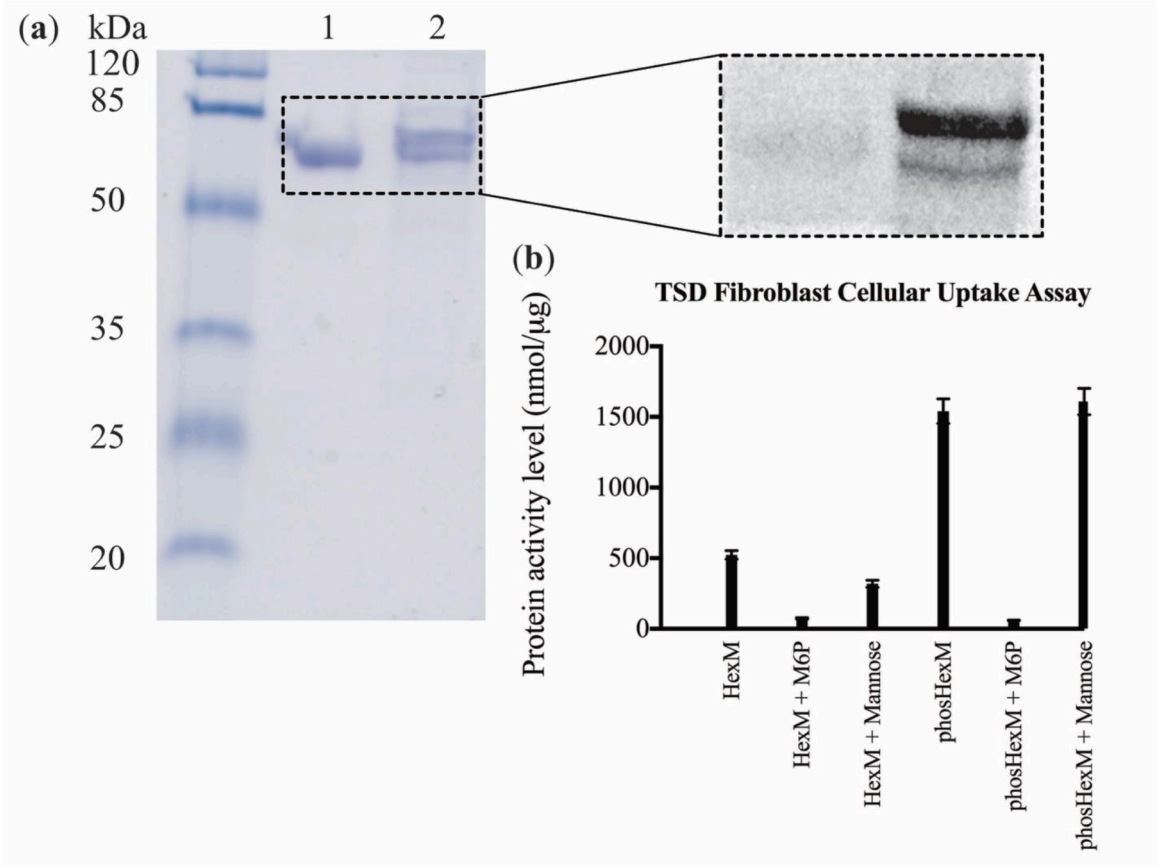

Fig. 4. Hyperphosphorylation of HexM by an engineered S1S3 GlcNac-1-phosphotransferase (S1S3 PTase) [16]. (a) SDS-PAGE gel of unmodified (lane 1) and hyperphosphorylated HexM (PhosHexM) (lane 2) with inset showing gel stained with Phospho-Tag, a fluorescent stain that selectively binds phosphate groups and clearly significant enhancement of HexM phosphorylation in the presence of the transferase. Unmodified HexM and PhosHexM were produced by HEKHexABKO-HexM cells, with the latter enzyme produced by cells that had also been transiently transfected with the S1S3 PTase expression plasmid [16]. (b) Generation of PhosHexM by the S1S3 PTase increases cellular of HexM uptake into TSD fibroblast cells. HexM activity is expressed as the ratio of the standardized MUGS activity versus total protein concentration of each cell lysate sample.

mediated by M6P receptors, as it is for HexM that has not been modified by co-expression with the transferase (Figure 4**b**).

3.4. MS data of HexM verified one similar glycosylation site as HexA

Mass spectrometry (MS) analysis of HexM found high mannosylated N-linked glycan structures on Asn157 on the μ-subunit homodimer, corresponding to a known glycosylated residue on the α-subunit of human HexA. Attempts to analyze the other known sites on the α-subunit (N115 and N296) by MS were unsuccessful. The proteolytic enzyme GluC was chosen over trypsin as the latter produces peptides too large for MS analysis. For HexA and HexM, Glu-C leads to the three following peptides containing glycosylation sites: SVE^{115}**N**YTLTINDDQCLLLSE (MW 2169), GTFFI^{157}**N**KTE (MW 1055) and FDTPGHTLSWGPGIPGLLTPCYSGSEPSGTFGPVNPSL^{295}**N**NTYE (MW 4463) for HexM and HexA. The first and third peptides were not observed at all by MS at their non-glycosylated MW values, which could indicate glycosylation. However as shown in Figure 5, the addition of a Man7 glycan structure adds 1541 in mass to the peptide GTFFI**N**KTE, which would mean m/z 3711 and 6005 for the Man-7 versions of the first and third peptides, respectively, for which there was no clear observation. Overall, the use of Glu-C was conclusive only for the glycosylation and phosphorylation of GTFFI**N**KTE. Table 1 gives the compositions of the high mannose glycans, which were the same in HexM and HexA (also see Figure 5).

4. Discussion

For ERT to be successful, the therapeutic enzyme must be stable and its production scalable to gram-level quantities. Given the high level HexM production we were able to achieve using even a small FiberCell bioreactor compared to basic culture flasks, we posit that a larger mammalian cell suspension bioreactor system could readily produce gram-scale quantities of the enzyme for ERT trials at reasonable cost. Indeed, we were able to generate over half a gram of active HexM using a small FiberCell bioreactor cartridge (C2011) that we let operate over several months. Since HexM is expressed from a single open reading frame and forms a highly stable homodimer that is not prone to subunit exchange that is typical of HexA [25], HexM was remarkably easy to purify at scale.

The *piggyBac* transposon-based expression system [15] enabled remarkable levels of HexM expression when combined with the Fibercell system and this prompted us to use the system to generate an expression system for human HexA. Though the purification scheme was more complex due the generation of three possible isoforms during expression (HexA, HexB and HexS), milligram yields of pure and active HexA are possible using the system. This expression system will now enable new small molecule screening and structure-based design efforts to advance pharmacological chaperone discovery that could be used as stand-alone treatments for later-onset forms of GM2 gangliosidoses or possibly combined with HexM-based ERT [22].

Though we had previously found that HexM is endocytosed to the lysosomes of Tay-Sachs disease fibroblast cells in a M6P-dependent

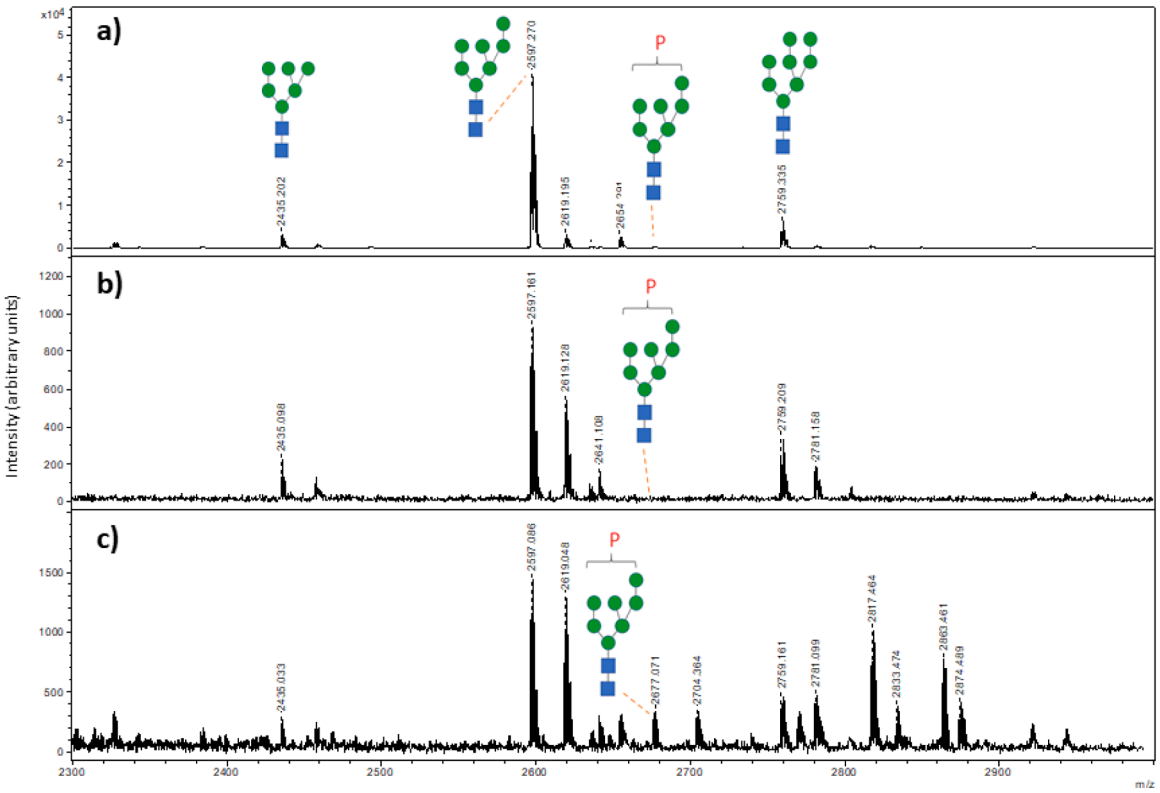

Fig. 5. MALDI-MS spectra of glycosylated peptide GTFFINKTE from the Glu-C digestion of (a) HexA, (b) HexM and (c) PhosHexM, showing the presence of high mannose species and enhanced phosphorylation.

Table 1
MALDI-MS analysis of phosphorylation of high mannose N-linked glycosylation sites of recombinant HexA and recombinant HexM. [a] The presence of phosphorylation, denoted by the letter P, was found at very low signal intensities for both protein samples. PhosHexM showed a higher level of phosphorylation, see Figure 5 in discussion. H = hexose (mannose), N = N-acetylglucosamine.

Glycosylation site	**HexM and HexA**
N157	H6N2
	H7N2
	H7N2P[a]
	H8N2

manner [12], mass spectrometry (MS) analysis (as described [26]) of Glu-C digests of HexM revealed that at least one of the three N-glycans is only ~1-2 % (**Figure 5b**), similar to what is observed in HexA (**Figure 5a**). Glycoproteomic experiments, i.e. glycopeptide analyses were carried out in order to observe both the glycan structures and their respective glycosylation sites. Three known sites exist in the μ-subunit of HexM: N115, N157, and N295. Their equivalents in the α-subunit of HexA are N115, N157, and N296. Mass spectrometric analysis of the Glu-C digest of PhosHexM clearly shows enhancement in phosphorylation to a level of about 20% (**Figure 5c**) at site N157. These levels are only qualitative representations, as part of the M6P O-phosphate bonds may hydrolyze under acidic MALDI conditions.

Phosphorylation of glycan structures on HexM was only detected for ^{157}N in this study. However, attempts to use the less specific enzyme pepsin to digest HexA and HexM led to the possible observation of complex glycan structures on ^{115}N and ^{295}N in HexA, although these results could not be repeated and were not reproducible in the case of HexM. Pepsin did, however, provide a clear picture for high mannose and phosphorylation of ^{157}N, owing to the glycopeptide **I**NKTEIEDF. Pepsin results will be presented in a separate report, as investigations are still ongoing.

Given the apparent low level of phosphorylation observed in HexM, it appeared cellular uptake of HexM could be improved by increasing mannose phosphorylation, which could significantly reduce the amount of HexM required to achieve therapeutic efficacy. A common issue facing large-scale production of recombinant enzyme used for lysosomal ERT is inadequate *in cellulo* phosphorylation. Two factors appear to contribute to this problem: 1) the endogenous levels of glycosylating and phosphorylating enzymes are incommensurate with the massive artificial increase in recombinant enzyme production that occurs in the mammalian cell expression system, and 2) the recombinant protein is simply a poor substrate for high-mannose phosphorylation [16]. Phosphorylation of high mannose sugars on glycans attached to lysosome-bound proteins is carried out by the Golgi enzyme GlcNAc-1-PT, which selectively transfers GlcNAc-1-P from UDP-GlcNAc to mannose sugars on high mannose-type N-linked glycans of lysosomal enzymes [27]. GlcNAc is subsequently removed by N-acetylglucosamine-1-phosphodiester-N-acetylglucosaminidase (NAGPA) [28], revealing M6P moieties that target the enzyme to the lysosome via M6P receptor proteins in the *trans*-Golgi apparatus [29]. M6P receptors found on the cell surface can also sequester exogenously provided M6P tagged enzyme to the lysosome, which enables ERT [11].

To enhance the phosphorylation of lysosomal enzymes, we recently generated a highly active and promiscuous variant of GlcNac-1-PT (S1S3 PTase) that enhances the phosphorylation of lysosomal proteins [16]. Co-expression of HexM with S1S3 PTase yielded hyperphosphorylated HexM (PhosHexM) that was taken up by TSD fibroblast cells three times greater than HexM expressed in the absence of the engineered transferase. This exciting result demonstrates the utility of using the engineered transferase to enhance the potential of HexM as an ERT therapy by markedly improving its uptake into deficient cells. Notably, there is a widespread distribution of neuronal cells that possess mannose-6-phosphate receptors present throughout the central nervous

system (CNS) [30], highlighting the usefulness of the mannose-6-phosphate pathway in facilitating the delivery of exogenously provided HexM.

Taken together, the scalable production of pure HexM and our ability to hyperphosphorylate the enzyme by co-expressing it with S1S3 PTase now positions HexM for further analysis as a therapeutic enzyme. Hyperphosphorylation of HexM adds considerable potential to its therapeutic position and builds upon the HexM strategy and could enhance other similar approaches to treating Tay-Sachs and Sandhoff disease [31]. A number of animal models of Tay-Sachs and Sandhoff disease are now available to test the feasibility of HexM as a ERT to manage these diseases [32]. However, penetration of the blood-brain barrier (BBB) and potential immunogenicity issues remain as significant obstacles for ERT approaches that attempt to address lysosomal disorders affecting the CNS, including Tay-Sachs and Sandhoff disease. ICV administration of drugs is an accepted clinical procedure that bypasses the BBB to deliver therapeutic enzymes directly into the CNS [33–35] and we are now exploring this mode of delivery of HexM into mouse models of Tay-Sachs and Sandhoff disease, as has been done for other mouse models of lysosomal storage disorders [35]. Nevertheless, ICV administration is highly invasive and poses risk of infection and other complications [34]. In contrast, exciting advancements in exploiting receptor-mediated transcytosis pathways to transfer lysosomal enzymes across the BBB using peptide or protein-based BBB shuttles provide promising alternatives to ICV administration [36–39]. Given the options that are emerging for delivery of therapeutic molecules to the CNS, we aim to explore these delivery options to provide HexM as a therapeutic option to manage Tay-Sachs and Sandhoff disease.

Conflict of Interest

C.D. and S.K. are co-founders of M6P Therapeutics and have equity interests in the company. B.L.M. is a co-inventor on a patent protecting the sequence and potential uses of HexM.

Declaration of Competing Interests

The authors declare the following financial interests/personal relationships which may be considered as potential competing interests:

Stuart Kornfeld reports a relationship with M6P Therapeutics that includes: equity or stocks. Cuong Do reports a relationship with M6P Therapeutics that includes: equity or stocks. Brian Mark and Don Mahuran has patent #US 10400227 B2 issued to M6P Therapeutics (non-exclusive) and New Hope Research Foundation (non-exclusive). Stuart A. Kornfeld, Balraj Doray, Wang Lee, Lin Liu has patent #US10907139B2 pending to M6P Therapeutics.

Acknowledgments

This research was funded by grants from the Canadian Glycomics Network (Catalyst grant) and the Canadian Institutes of Health Research (PJT-162414) to B.L.M, B.T-R and H.P. The HEKHexABKO and HEKHexABKO-HexM cell lines were provided by Dr. Don Mahuran, SickKids Hospital, Toronto, Canada. The authors thank Duc Minh Nguyen and Tyler Tran for performing the initial mass spectrometry experiments on HexA and HexM.

Supplementary materials

Supplementary material associated with this article can be found, in the online version, at doi:10.1016/j.bbadva.2021.100032.

References

[1] R.A. Gravel, M.M. Kaback, R.L. Proia, K. Sandhoff, K. Suzuki, K. Suzuki, The GM2 gangliosidoses, in: C.R. Scriver, A.L. Beaudet, W.S. Sly, D. Valle (Eds.), Metabolic and Molecular Bases of Inherited Disease, 8th ed., McGraw-Hill, New-York, 2001, pp. 3827–3876.

[2] E. Conzelmann, K. Sandhoff, Purification and characterization of an activator protein for the degradation of glycolipids GM2 and GA2 by hexosaminidase A, Hoppe-Seylers Zeitschrift Für Physiol, Chemie 360 (1979) 1837–1849.

[3] M.J. Virgolini, C. Feliziani, M.J. Cambiasso, P.H. Lopez, M. Bollo, Neurite atrophy and apoptosis mediated by PERK signaling after accumulation of GM2-ganglioside, Biochim. Biophys. Acta - Mol. Cell Res. 1866 (2019) 225–239, https://doi.org/10.1016/j.bbamcr.2018.10.014.

[4] K. Sandhoff, K. Harzer, Gangliosides and gangliosidoses: Principles of molecular and metabolic pathogenesis, J. Neurosci. 33 (2013) 10195–10208, https://doi.org/10.1523/JNEUROSCI.0822-13.2013.

[5] E. Conzelmann, K. Sandhoff, Partial enzyme deficiencies: residual activities and the development of neurological disorders, Dev. Neurosci. 6 (1983) 58–71.

[6] E. Andermann, C.R. Scriver, L.S. Wolfe, L. Dansky, F. Andermann, Genetic variants of Tay-Sachs disease: Tay-Sachs disease and Sandhoff's disease in French Canadians, juvenile Tay-Sachs disease in Lebanese Canadians, and a Tay-Sachs screening program in the French-Canadian population, Prog. Clin. Biol. Res. 18 (1977) 161–188.

[7] G. Sillon, P. Allard, S. Drury, J.B. Rivière, I. De Bie, The incidence and carrier frequency of Tay-Sachs disease in the French-Canadian population of Quebec based on retrospective data from 24 years, 1992–2015, J. Genet. Couns. 29 (2020) 1173–1185, https://doi.org/10.1002/jgc4.1284.

[8] G.M. Petersen, J.I. Rotter, R.M. Cantor, L.L. Field, S. Greenwald, J.S. Lim, C. Roy, V. Schoenfeld, J.A. Lowden, M.M. Kaback, The Tay-Sachs disease gene in North American Jewish populations: Geographic variations and origin, Am. J. Hum. Genet. 35 (1983) 1258–1269.

[9] P.J. Meikle, J.J. Hopwood, A.E. Clague, W.F. Carey, Prevalence of lysosomal storage disorders, J. Am. Med. Assoc. 281 (1999) 249–254, https://doi.org/10.1001/jama.281.3.249.

[10] G.H.B. Maegawa, T. Stockley, M. Tropak, The natural history of juvenile or subacute GM2 gangliosidosis: 21 New cases and literature review of 134 previously reported, Pediatrics 120 (2006) 936, https://doi.org/10.1542/peds.2007-0343.

[11] M. Solomon, S. Muro, Lysosomal Enzyme Replacement Therapies: Historical Development, Clinical Outcomes and Future Perspectives, Adv. Drug Deliv. Rev. 118 (2017) 109–134, https://doi.org/10.1016/j.addr.2017.05.004.Lysosomal.

[12] M.B. Tropak, S. Yonekawa, S. Karumuthil-Melethil, P. Thompson, W. Wakarchuk, S.J. Gray, J.S. Walia, B.L. Mark, D. Mahuran, Construction of a hybrid β-hexosaminidase subunit capable of forming stable homodimers that hydrolyze GM2 ganglioside in vivo, Mol. Ther. - Methods Clin. Dev. 3 (2016) 15057, https://doi.org/10.1038/mtm.2015.57.

[13] M.J. Lemieux, B.L. Mark, M.M. Cherney, S.G. Withers, D.J. Mahuran, M.N. G. James, Crystallographic structure of human β-hexosaminidase A: interpretation of Tay-Sachs mutations and loss of GM2 ganglioside hydrolysis, J. Mol. Biol. 359 (2006) 913–929, https://doi.org/10.1016/j.jmb.2006.04.004.

[14] B.L. Mark, D.J. Mahuran, M.M. Cherney, D. Zhao, S. Knapp, M.N.G. James, Crystal structure of human β-hexosaminidase B: understanding the molecular basis of Sandhoff and Tay-Sachs disease, J. Mol. Biol. 327 (2003) 1093–1109, https://doi.org/10.1016/S0022-2836(03)00216-X.

[15] Z. Li, I.P. Michael, D. Zhou, A. Nagy, J.M. Rini, Simple piggyBac transposon-based mammalian cell expression system for inducible protein production, Proc. Natl. Acad. Sci. U. S. A. 110 (2013) 5004–5009, https://doi.org/10.1073/pnas.1218620110.

[16] L. Liu, W.S. Lee, B. Doray, S. Kornfeld, Engineering of GlcNAc-1-phosphotransferase for production of highly phosphorylated lysosomal enzymes for enzyme replacement therapy, Mol. Ther. - Methods Clin. Dev. 5 (2017) 59–65, https://doi.org/10.1016/j.omtm.2017.03.006.

[17] M. Meyerson, C.M. Counter, E.N. Eaton, L.W. Ellisen, P. Steiner, S.D. Caddle, L. Ziaugra, R.L. Beijersbergen, M.J. Davidoff, L. Qingyun, S. Bacchetti, D.A. Haber, R.A. Weinberg, hEST2, the putative human telomerase catalytic subunit gene, is up- regulated in tumor cells and during immortalization, Cell 90 (1997) 785–795, https://doi.org/10.1016/S0092-8674(00)80538-3.

[18] Y. Hou, R. Tse, D.J. Mahuran, Direct determination of the substrate specificity of the α-active site in heterodimeric β-hexosaminidase A, Biochemistry 35 (1996) 3963–3969, https://doi.org/10.1021/bi9524575.

[19] R. Sharma, H. Deng, A. Leung, D. Mahuran, Identification of the 6-sulfate binding site unique to α-subunit-containing isozymes of human β-hexosaminidase, Biochemistry 40 (2001) 5440–5446, https://doi.org/10.1021/bi0029200.

[20] M.L. Shulman, V.A. Kulshin, A.Y. Khorlin, A continuous fluorimetric assay for glycosidase activity: Human N-acetyl-β-d-hexosaminidase, Anal. Biochem. 101 (1980) 342–348, https://doi.org/10.1016/0003-2697(80)90198-0.

[21] P. Hechtman, F. Kaplan, J. Bayleran, B. Boulay, E. Andermann, M. De Braekeleer, S. Melancon, M. Lambert, M. Potier, R. Gagne, E. Kolodny, C. Clow, A. Capua, C. Prevost, C. Scriver, More than one mutant allele causes infantile Tay-Sachs disease in French-Canadians, Am. J. Hum. Genet. 47 (1990) 815–822.

[22] M.B. Tropak, S.P. Reid, M. Guiral, S.G. Withers, D. Mahuran, Pharmacological enhancement of β-hexosaminidase activity in fibroblasts from adult Tay-Sachs and Sandhoff patients, J. Biol. Chem. 279 (2004) 13478–13487, https://doi.org/10.1074/jbc.M308523200.

[23] R. Sharma, S. Bukovac, J. Callahan, D. Mahuran, A single site in human β-hexosaminidase A binds both 6-sulfate-groups on hexosamines and the sialic acid moiety of GM2 ganglioside, Biochim. Biophys. Acta - Mol. Basis Dis. 1637 (2003) 113–118, https://doi.org/10.1016/S0925-4439(02)00221-1.

[24] H.J. Kytzia, K. Sandhoff, Evidence for two different active sites on human β-hexosaminidase A. Interaction of G(M2) activator protein with β-hexosaminidase A, J. Biol. Chem. 260 (1985) 7568–7572.

[25] D. Mahuran, J.A. Lowden, The subunit and polypeptide structure of hexosaminidases from human placenta, Can. J. Biochem. 58 (1980) 287–294, https://doi.org/10.1139/o80-038.
[26] E. Komatsu, M. Buist, R. Roy, A.G. Gomes de Oliveira, E. Bodnar, A. Salama, J. P. Soulillou, H. Perreault, Characterization of immunoglobulins through analysis of N-glycopeptides by MALDI-TOF MS, Methods 104 (2016) 170–181, https://doi.org/10.1016/j.ymeth.2016.01.005.
[27] M.L. Reitman, S. Kornfeld, Lysosomal enzyme targeting. N-acetylglucosaminylphosphotransferase selectively phosphorylates native lysosomal enzymes, J. Biol. Chem. 256 (1981) 11977–11980, https://doi.org/10.1016/s0021-9258(18)43217-6.
[28] A. Varki, S. Kornfeld, Identification of a rat liver alpha-N-acetylglucosaminyl phosphodiesterase capable of removing "blocking" alpha-N-acetylglucosamine residues from phosphorylated high mannose oligosaccharides of lysosomal enzymes, J. Biol. Chem. 255 (1980) 8398–8401, https://doi.org/10.1016/s0021-9258(18)43507-7.
[29] H.D. Fischer, A. Gonzalez-Noriega, W.S. Sly, D.J. Morre, Phosphomannosyl-enzyme receptors in rat liver. Subcellular distribution and role in intracellular transport of lysosomal enzymes, J. Biol. Chem. 255 (1980) 9608–9615, https://doi.org/10.1016/s0021-9258(18)43435-7.
[30] C. Hawkes, S. Kar, Insulin-like growth factor-II/mannose-6-phosphate receptor: Widespread distribution in neurons of the central nervous system including those expressing cholinergic phenotype, J. Comp. Neurol. 458 (2003) 113–127, https://doi.org/10.1002/cne.10578.
[31] K. Kitakaze, Y. Mizutani, E. Sugiyama, C. Tasaki, D. Tsuji, N. Maita, T. Hirokawa, D. Asanuma, M. Kamiya, K. Sato, M. Setou, Y. Urano, T. Togawa, A. Otaka, H. Sakuraba, K. Itoh, Protease-resistant modified human β-hexosaminidase B ameliorates symptoms in GM2 gangliosidosis model, J. Clin. Invest. 126 (2016) 1691–1703, https://doi.org/10.1172/JCI85300.
[32] C.A. Lawson, D.R. Martin, Animal models of GM2 gangliosidosis: utility and limitations, Appl. Clin. Genet. 9 (2016) 111–120.
[33] M.I. Alam, S. Beg, A. Samad, S. Baboota, K. Kohli, J. Ali, A. Ahuja, M. Akbar, Strategy for effective brain drug delivery, Eur. J. Pharm. Sci. 40 (2010) 385–403, https://doi.org/10.1016/j.ejps.2010.05.003.
[34] J.L. Cohen-Pfeffer, S. Gururangan, T. Lester, D.A. Lim, A.J. Shaywitz, M. Westphal, I. Slavc, Intracerebroventricular delivery as a safe, long-term route of drug administration, Pediatr. Neurol. 67 (2017) 23–35, https://doi.org/10.1016/j.pediatrneurol.2016.10.022.
[35] S. Stroobants, D. Gerlach, F. Matthes, D. Hartmann, J. Fogh, V. Gieselmann, R. D'Hooge, U. Matzner, Intracerebroventricular enzyme infusion corrects central nervous system pathology and dysfunction in a mouse model of metachromatic leukodystrophy, Hum. Mol. Genet. 20 (2011) 2760–2769, https://doi.org/10.1093/hmg/ddr175.
[36] B. Oller-Salvia, M. Sánchez-Navarro, E. Giralt, M. Teixidó, Blood-brain barrier shuttle peptides: An emerging paradigm for brain delivery, Chem. Soc. Rev. 45 (2016) 4690–4707, https://doi.org/10.1039/c6cs00076b.
[37] A. Böckenhoff, S. Cramer, P. Wölte, S. Knieling, C. Wohlenberg, V. Gieselmann, H. J. Galla, U. Matzner, Comparison of five peptide vectors for improved brain delivery of the lysosomal enzyme arylsulfatase A, J. Neurosci. 34 (2014) 3122–3129, https://doi.org/10.1523/JNEUROSCI.4785-13.2014.
[38] L. Ou, M.J. Przybilla, B. Koniar, C.B. Whitley, RTB lectin-mediated delivery of lysosomal α-L-iduronidase mitigates disease manifestations systemically including the central nervous system, Mol. Genet. Metab. 123 (2018) 105–111, https://doi.org/10.1016/j.ymgme.2017.11.013.
[39] D. Wang, S.S. El-Amouri, M. Dai, C.Y. Kuan, D.Y. Hui, R.O. Brady, D. Pan, Engineering a lysosomal enzyme with a derivative of receptor-binding domain of apoE enables delivery across the blood-brain barrier, Proc. Natl. Acad. Sci. U. S. A. 110 (2013) 2999–3004, https://doi.org/10.1073/pnas.1222742110.